Strathprints Institutional Repository

This version is available at http://strathprints.strath.ac.uk/52517/

Modern NMR Pulse Sequences in

Pharmaceutical R & D

John A. Parkinson

WestCHEM, Department of Pure and Applied Chemistry NMR Spectroscopy Facility, University of Strathclyde Glasgow G1 1XL.

Abstract

NMR pulse sequences are surveyed for solution-state methods that serve as typical, robust techniques in pharmaceutical or chemical NMR laboratories. Attention is drawn to up-to-date methods capable of enhancing sensitivity, resolution and information content. Sequences range from those used for pulse calibration and field homogeneity adjustment, through one- and two-dimensional homo- and hetero-nuclear methods for solution phase work. Techniques used for editing, resolving and simplifying data are highlighted and extensive use is made of sequence diagrams to present the basic structure of each pulse sequence in pictorial form. Where appropriate, descriptions of each sequence and some examples of data are provided and attention drawn to the advantages of using each technique.

1 INTRODUCTION

Commercial NMR equipment evolution owes much to the demands imposed by users requiring ever more sophisticated experimental capabilities. One outcome is a bewildering array of pulse sequences, which are often subtle variations or improvements on a particular theme. They may depend on frequency-, band- or spatially-selective excitation, entail diverse homo- and/or hetero-nuclear frequency correlation schemes or use editing methods to simplify and enhance the resulting data. Across the breadth of all NMR-related disciplines, such diversity can be overwhelming and confusing. In this article I have selected pulse sequences that stand out as those most regularly used by NMR practitioners or which merit special emphasis owing to their future promise in routine spectroscopy. The methods yield rich information, are mostly straightforward to implement and show robustness when applied in a modern spectrometer context. These are essentials in unsupervised, robotic settings. The methods yield data for understanding small molecules, their structures, behaviours and interactions, whether as pure materials, contaminants or components within complex mixtures. Here I consider the sequences, use some examples of data they produce and describe how they can be adjusted to function optimally.

2 INITIAL SAMPLE ADJUSTMENTS

Sample set-up including modern approaches to optimizing magnetic field homogeneity (shimming) and calibration of the ^{1}H 90° pulse are important initial considerations in a solution-phase context.

2.1 Shimming

The process of field optimization has evolved from one based on lock signal measurement using lengthy iterative simplex procedures to the use of field mapping linked with resonance lineshape analysis and optimization,[1] which adds value to the rapid mapping procedure and provides an approach that virtually guarantees optimized field homogeneity under full automation (*see* emrstm1228). The classical gradient echo imaging sequence (**Figure 1**) exploits the z-gradient coil of a modern solution-phase NMR probe for one-dimensional field mapping and in combination with room temperature x and y non-spin shims for three-dimensional field mapping.

(Insert **Figure 1** here).

Two experiments generate data using the echo periods TE_1 and TE_2, the difference between the resulting data yielding a phase map. When compared with reference data, the process allows shim values to be directly set, providing a more optimized field. The process is iterative but takes as little as 10-20 s for 1D field mapping and a little longer (10-15 minutes) for complete 3D field mapping. Rapid 1D field mapping with lineshape optimization is ideally suited to unsupervised sample analysis, relying as it does on one dominating resonance in the spectrum. For this reason, the lock solvent deuterium signal is often used in this process.

2.2 ^{1}H 90° Pulse Calibration

Accurate calibration of the ^{1}H 90° pulse has been traditionally measured by a time consuming single pulse-acquire sequence with an array of pulse lengths.[2] This process is incompatible if required as a feature of every data acquisition under automation. In an unsupervised setting, pulse mis-setting results in non-optimized data. The modern alternative relies on measuring

nutation of the magnetization vector in a rapid, single shot.[3] The pulse sequence, akin to homo-nuclear decoupling, uses a train of pulses between each of which is acquired a single data point. The resulting sinusoidal data are Fourier transformed generating two resonances (for a predominating response) separated by twice the nutation frequency, Δv. Data are acquired during the dwell period with a duty cycle, d, from which the 90° pulse is calculated according to $pw_{90}=d/(2\Delta v)$. The method can be fully automated and owing to its speed, can in theory be incorporated into all data acquisitions. In this way, all pulse sequences can be fully optimized for sensitivity and performance under full automation regardless of sample type or refined probe tuning, thus substantially improving data quality and reliability.

3. ONE-DIMENSIONAL METHODS

The single pulse-acquire sequence is the most basic NMR experiment. Delivered as a short burst (8-12 μs) of radiation at high power (typically in the order of 10-20 W), the pulse creates a non-crafted excitation profile across the expected data acquisition bandwidth. Pulse length is adjusted to yield magnetization vector rotation of any desirable angle. A small rotation angle of typically 30° is often desirable to promote restoration of equilibrium magnetization.

3.1. Editing Schemes

Crafted NMR data falls under the guise of frequency specific- or band-selective procedures.

3.1.1   Frequency- and band-selective data acquisition

Similar to the single pulse-acquire scheme, frequency- or band-selective sequences make use of low power, long duration tailored pulses that narrow the excitation bandwidth to the region of interest, whether this be a single resonance (frequency-selective) or a frequency region (band-selective) (*see* emrstm0493). Single resonance selection alone has limited use but is suitable for assessing pulse power calibration and frequency selectivity. A range of pulse shapes have been developed which serve very wide ranging purposes (*see* emrstm0486).

3.1.2   1D-TOCSY

The power of tailored excitation emerges when combined with sequences for revealing correlations between related spins. For instance, 1D-TOCSY is useful in resolving data when signal overlap is extensive in some regions of data and resolved in others. Isolated signals are selected and manipulated to reveal spin-system partners at high digital resolution. The sequence is represented here in two forms (**Figure 2**). The benefit of incorporating procedures to eliminate, in a single transient, interfering effects caused by zero-quantum coherence (*see* emrstm1257) are also illustrated.

(Insert **Figure 2** here)

An excitation construct is used to cleanly select the resonance from which magnetization is propagated to the remainder of the spin-system nuclei. Isotropic mixing by the DIPSI-2 spin-lock sequence is preferred for more efficient mixing of the magnetization and the use of lower pulse powers across the bandwidth of interest compared with non-isotropic mixing sequences.[4] The basic pulse sequence (**Figure 2a**) yields results typical of those shown (**Figure 3b**).

(Insert **Figure 3** here)

Interference from zero-quantum coherence ultimately contributes anti-phase magnetization to the observed signal. Unwanted dispersive signals add to the pure absorption lineshape, playing havoc with the data. The popular alternative (**Figure 2b**) engages adiabatic pulses over weak field gradients to dephase unwanted zero-quantum coherence before and after the spin-lock period.[5] Z-filter delays of typical duration 2-3 ms are set to different values to avoid refocusing magnetization from unwanted coherence pathways. The cleaner result (**Figure 3c**) arises solely from pure absorption lineshape.

3.1.3   1D-NOESY and 1D-ROESY

Tailored excitation has also benefited the development of the NOE experiment, which has evolved from the truncated driven, difference method, requiring multiple transients to average out subtraction artefacts, to the modern single- or double pulsed field gradient spin-echo (DPFGSE) approach that incorporates the same zero-quantum suppression construct described for 1D-TOCSY (**Figure 4**) (*see* emrstm0350).

(Insert **Figure 4** here)

In the preparation period, the double pulsed field gradient spin-echo (DPFGSE) feature cleanly selects only resonances of interest. A mixing pulse inverts the resulting spin magnetization from which evolves the NOE during the mixing period. The adiabatic 180˚ pulse over a weak field gradient eliminates the lineshape-distorting effects of zero quantum coherence, which is then followed by a purging gradient and a 90˚ read pulse. The experiment works with relatively few transients compared with its historical counterpart.

Variations on this theme exist which, for longer mixing times, require the distribution of hard 180˚ inversion pulses surrounded by opposing gradients within the mixing period to purge responses from unwanted coherences. 1D-NOESY yields transient NOEs and is appropriate for also detecting chemical exchange processes as is the case with 2D-NOESY.

1D-ROESY requires adaptation of the 1D-NOESY sequence by incorporating a spin-lock construct to replace the mixing sequence $90˚$-τ_m-$90˚$. In all other respects the sequence is the same but care must be taken to reduce the influence of unwanted TOCSY responses (*see* emrstm0573). As an alternative, 1D-ROESY may better be derived from the robust 2D-EasyROESY as further described under section 4.2.2 ROESY.

Techniques such as 1D-NOESY, -TOCSY and –ROESY when combined form homo-nuclear concatenated sequences that propagate magnetization transfer from spin to spin *via* dipolar-, or spin/spin-coupling and/or chemical exchange mechanisms. Such spliced sequences can use similar constructs e.g. 1D-TOCSY-TOCSY or different constructs e.g. 1D-TOCSY-ROESY. The combined methods help when teasing out assignments but are less robust in an automated setting.[6]

3.1.4   *Homonuclear Broadband Decoupling*

Spin-spin coupling provides critical information about related nuclei but removing the resonance-spreading effects of *J*-coupling can be desirable to simplify NMR data and improve resolution. This is readily achieved in broadband hetero-nuclear decoupling for spin interactions between different types of nuclei such as ^1H and ^{13}C. However, broadband homo-nuclear decoupling is an entirely different avenue, having proved to be a significant historical challenge for ^1H NMR spectroscopy. Theoretically the aim is to produce ^1H-$\{^1H\}_{BB}$ NMR

data. Generating the skyline projection from fully processed 2D *J*-resolved NMR spectra (*see* emrstm1048 and emrstm0579) is one way of visualizing this but the results are unsatisfactory owing to poor signal resolution and variable signal amplitude unrelated to true integral values. Other related methods have been published in the more recent literature in a bid to counter the integral issue but these prove unwieldy for routine practical use.[7] The prize for creating ^{1}H-$\{^1$H$\}_{BB}$ NMR data is increased signal resolution for no increase in static magnetic field strength. If achieved with reliable signal integration at full sensitivity, a new NMR milestone will have been reached. This goal is now within sight for routine use in an automated laboratory context. Two categories of pulse sequence now exist which go some way towards achieving this, namely full ^{1}H sensitivity, homo-nuclear band-selective decoupled (HOBS) methods[8] and reduced ^{1}H sensitivity, homo-nuclear broadband decoupled (Pureshift) methods.[9,10] The former relies on band-selection for the special case where signals in the selected region do not *J*-couple to one another but rather to resonances beyond the selected region. This HOBS approach is ideally suited to biopolymers including peptides, proteins and nucleic acids whose NMR spectra are regionalized owing to the polymeric nature of the molecules concerned. One-dimensional HOBS spectra can be produced by the sequence shown (**Figure 5**) from which a wide variety of other related sequences may be constructed.

(Insert **Figure 5** here)

The region-selective preparation construct uses a band-selective 180˚ pulse. The acquisition stage collects data non-continuously as data packets. Between data collection, gradient-bracketed hard 180˚ and band-selective 180˚ pulses are inserted. These components repeatedly refocus ^{1}H spin-spin couplings for those resonances in the band-selected region of

interest for the special coupling condition described for biopolymers. Segments of FID are acquired for limited periods of up to ~ 30 ms (approximating to $1/3J_{HH}$). Chemical shifts evolve much faster than J-couplings meaning that chemical shift information is laid down in the FID segments while the effects of J-coupling are regularly removed through refocusing. A draw-back to this technique is that during these refocusing periods, T_2-relaxation is active leading to some discontinuities in the FID yielding spectral artefacts. Looping the acquisition stage yields a FID with acquisition duration adequate for high-resolution spectra with acceptable lineshape (**Figure 6b**).

(Insert **Figure 6** here).

Full proton sensitivity is desirable and achieved for HOBS but the special coupling conditions make it less attractive for general purpose application, despite it being readily implemented under full automation for biopolymers. Related procedures for generating ^{1}H-{^{1}H}$_{BB}$ NMR data are available using several approaches albeit with reduced sensitivity.[9,10,11] For routine use, the continuous (instantaneous) Pureshift data acquisition scheme is attractive.[10] The principal difference between this and HOBS lies in the application of a narrow band, frequency selective shaped inversion pulse applied during a weak pulsed field gradient. The latter spatially encodes spin magnetization along the length of the NMR sample. If the field gradient is adjusted so that the entire ^{1}H NMR spectrum is excited by the selective inversion pulse along the sample length during the preparation period, a very acceptable high-resolution, broadband decoupled ^{1}H NMR spectrum can be generated. Data quality compared with standard ^{1}H NMR spectra is affected in two ways. Firstly, sensitivity is compromised owing to the spatial encoding: only a fraction (~ 1%) of spins contribute to any particular signal. Secondly, the technique does not tolerate strong J-coupling. Alternative

proposals for overcoming this have been published in a bid to address the insensitive nature of the technique.[11] These methods show merit in simplifying ^{1}H NMR spectra and their improved resolution 2D analogues are also promising.[12,13,14]

3.1.5 Diffusion- and T_2-editing

Diffusion and relaxation characteristics can also be used to simplify NMR data. Motional properties of molecules are exploited using diffusion ordered spectroscopy (DOSY), especially for studying mixtures of molecules whose size, shape and molecular weights vary with respect to one another (*see* emrstm1048). Classical diffusion experiments (*see* emrstm0118 and emrstm0119) use pulsed field gradients to label nuclei with their physical location in a sample. The diffusion period, Δ, is followed by a gradient refocusing construct that removes the spatial encoding. Diffusion of individual molecules during Δ causes the recovered magnetization to yield a lower than maximum response. A function of sample temperature, viscosity and the so-called friction factor, diffusion relies on molecular size, shape and weight. In the context of complex mixtures of small and large molecules, a diffusion filter applied at the start of a pulse sequence draws out signals exclusively from large molecules such as proteins at the expense of those from small molecules. Similarly T_2-filtering disposes of responses from large molecules to reveal more clearly those resonances from small molecules. Differences in T_2 relaxation time constants for different types of molecules are exploited using the classical Carr-Purcell-Meiboom-Gill (CPMG) sequence, which repeatedly refocuses chemical shift evolution by looping through a spin-echo sequence for a defined period of time during which T_2 relaxation acts (**Figure 7**).

(Insert **Figure 7** here)

Here τ is short (1-2 ms) compared with $1/J_{HH}$. *J*-modulation of signals occurs during the spin-echo period and may be minimized but is not altogether eliminated using this sequence. The unwanted effect from r.f. heating caused by the short duty cycle arising from multiple spin-echoes also degrades data quality. To compensate, the introduction of a *J*-refocusing 90˚ pulse between two spin-echo periods (**Figure 7b**) removes both *J*-modulation artefacts and allows the delay period τ to be extended by at least an order of magnitude thus reducing the r.f. load. With n > 1, this PROJECT (Periodic Refocusing of *J* Evolution by Coherence Transfer)[15] sequence gives NMR spectra with clean multiplet structures while delivering broad background resonance suppression (**Figure 8**).

(Insert **Figure 8** here)

3.2 **Solvent Suppression**

Samples studied in protonated solvents or very dilute samples studied in deuterated solvents give intense solvent signals that must be attenuated in the ^{1}H NMR spectrum to improve digitization without compromising solute responses. Many solvent suppression schemes are available with choice governed by application. No catch-all method exists but instead, each has its own advantages, disadvantages and particular merits.

3.2.1 Presaturation

For routine use, presaturation, which is a solvent spin saturation technique, is the most straightforward, general purpose method typically used for handling aqueous samples. Solvent signal suppression operates by low powered, continuous r.f. irradiation at the solvent resonance frequency during the long relaxation period. Following the saturation period, the sequence can be constructed from a number of different features (**Figure 9**).

(Insert **Figure 9** here)

Variants are designed to improve the quality of solvent suppression while leaving solute signals untouched. For aqueous solutions, the solvent frequency at the mid-point of the spectrum is made coincident with the transmitter offset and adjusted to minimize residual solvent signal. For other solvents whose ^{1}H resonance frequencies may not coincide with the centre of the ^{1}H spectral window, alternative schemes are used or the frequency width of the spectrum extended and the transmitter offset frequency adjusted appropriately to coincide with the solvent resonance.

3.2.2   *Watergate and Double Pulsed Field Gradient Spin Echo (DPFGSE)*

Solvent suppression approaches that minimize saturation transfer effects suppress the solvent signal in a more tailored fashion. Basic Watergate (Water suppression through gradient tailored excitation, G_1-S-G_1, where $S \equiv$ "soft-180˚-hard-180˚") and G represents pulsed field gradient)[16] and excitation sculpting[17] (DPFGSE, G_1-S-G_1-G_2-S-G_2) are variations on similar themes. Provided the transmitter offset coincides with the solvent resonance, the sequences dephase and eliminate the solvent resonance while refocusing the solute resonances that do not coincide with the region near the transmitter offset. With the exception of this central frequency window, data are acquired with uniform excitation across the desired region. DPFGSE yields a better phase response compared with the original Watergate but at the expense of longer spin manipulation periods. Reducing soft pulse and gradient periods helps to minimize saturation transfer effects. Variations on these methods use binomial pulse trains to further shorten the duration of the method. These show excitation nulls at regular frequency intervals including at the centre of the ^{1}H NMR spectrum.[18] They are arguably less

robust techniques that require some user intervention to ensure optimal performance. Watergate and DPFGSE suppress the solvent signal during an echo period *after* the read pulse, which contrasts with presaturation, when solvent suppression occurs as the first event in the pulse sequence. When combined with 2D methods that make use of extended mixing periods (as in TOCSY, ROESY and NOESY), the excitation sculpting approach to suppressing the H_2O response is considered to yield superior benefits.

3.2.3   WET

WET makes use of frequency-shifted soft pulses and can be used together with simultaneous ^{13}C-decoupling during the soft pulse and data acquisition periods to reduce the intensity of ^{13}C satellite signals from organic solvents, which can interfere with solute responses.[19] The method is ideal in the context of protonated organic solvents. WET incorporates a train of soft-pulses followed by spoiling gradients. [13]C decoupling is applied using a second independent r.f. channel during each of the soft pulses. The procedure collapses the ^{13}C satellite response. When followed by a spoiling gradient, the combined solvent-selective pulse with simultaneous hetero-nuclear decoupling attenuates solvent signals from both [12]C- and ^{13}C-attached ^{1}H nuclei. The soft pulse can be tailored to suppress multiple resonances from the same solvent in one hit. A train of such pulses with gradients reinforces the suppression effect and eliminates excess solvent signal ahead of the read pulse (**Figure 10**). The net effect can be impressive in revealing solute resonances from behind ^{13}C satellite signals (**Figure 11**).

(Insert **Figure 10** here)

(Insert **Figure 11** here)

The sequence is particularly useful for reaction process monitoring with liquid chromatography-(LC) coupled NMR systems in which protonated organic solvents serve as the mobile phase (*see* emrstm1193).

3.3 Ligand Screening

NMR approaches to ligand screening against potential biological targets form a key stage in modern drug discovery and design and either focus on the biological target or the ligand. SAR-by-NMR (Structure-Activity-Relationship by NMR)[20] focuses on the biological receptor and uses ^{15}N-labelled protein titrated with small molecule drug candidates. Conclusions are drawn from differences in ^{1}H and ^{15}N chemical shifts in 2D [^{1}H, ^{15}N] HSQC NMR data acquired and compared for ligand-free and ligand-bound protein. In promising cases, the data allow the ligand binding site to be mapped on the receptor surface. The procedure is unsuitable for identifying candidate drugs or fragments by mixture screening from compound libraries and requires large quantities of ^{15}N-labelled protein target. Instead, diffusion-editing, NOE-pumping, Water-LOGSY and Saturation Transfer Difference (STD) methods are used. We focus here on Water-LOGSY and STD as the two more robust approaches to small molecule fragment screening.[21]

3.3.1   Saturation Transfer Difference (STD)[22]

STD provides a fragment screening method for weakly binding ligands with $K_{D} \sim 10$ mM. The process uses protein at concentrations well below the level of NMR detection, typically requiring 100 pmol of material. ^{1}H resonances from mixtures of small molecules added to this therefore dominate the NMR spectrum. A train of soft pulses applied for 1–2 s selectively saturates the δ^{1}H = 0.0 to -1.0 ppm resonance region occupied only by unseen protein

responses. Saturation propagates quickly by spin-diffusion to all protein ^{1}H spins and to any bound ligand, regardless of how transient the binding event is. Spin saturation is then carried with any binding ligand upon its release into free solution. Control data, in which soft pulses are applied far off resonance, are used along with the on-resonance saturation data to generate difference spectra that only show responses for ligands which bind to the protein target. The approach can be thought of as a special case of presaturation.

3.3.2   Water-LOGSY

Water-LOGSY (Water-Ligand Observed by Gradient SpectroscopY, **Figure 12**)[23,24] also transfers magnetization to ligands by spin-diffusion but the mechanism occurs between water and the protein-ligand complex. It relies on chemical exchange and NOE processes associated with bulk water, water associated with the ligand binding site and labile protons within the protein. The water resonance is cleanly selected using the first section of the pulse sequence. The mixing time, τ_m, typically of the order of 1–2 s, promotes magnetization transfer from water to ligands that are in exchange with the protein binding site. A 180° pulse midway into the mixing period suppresses unwanted artefacts. The water flip-back pulse applied at the end of the mixing period maintains the majority of water magnetization along the z-axis during acquisition and relaxation delays so that pulse sequence repetition rates can be accelerated. A DPFGSE scheme is applied following the read pulse to cleanly suppress residual solvent magnetization. The resulting one-dimensional spectra report on protein-bound species as positive signals and non-interacting species as negative signals.

(Insert **Figure 12** here)

3.4 Pulse Sequences for ^{13}C NMR Spectroscopy

Although the most sensitive and obvious approach to analysing organic molecules in solution is by ^{1}H NMR spectroscopy, the framework of such molecules is by definition carbon-based. The 2D methods described in later sections are powerful procedures by which bond connectivity through ^{1}H and ^{13}C spin networks can be established. Despite this, there remains an attraction towards direct observation of ^{13}C-{^{1}H} NMR data, partly as a response to the need to observe NMR signals from quaternary carbons at high resolution and partly through cryoprobe development optimized for maximum^{13}C sensitivity.

3.4.1 DEPTQ

DEPTQ[25] is a more recent addition to the J-MOD or Attached Proton Test (APT)[26], DEPT and INEPT sequences commonly used to edit ^{13}C spectra on the basis of spin multiplicity (*see* emrstm0398). DEPTQ improves data quality and robustness over other methods by inclusion of hetero-nuclear adiabatic 180° inversion pulses[27] (**Figure 13**).

(Insert **Figure 13** here)

This makes DEPTQ ideal for direct ^{13}C data acquisition in a high-throughput context. Saturation of protons during the relaxation period builds the ^{1}H-^{13}C NOE for enhancement of ^{13}C signal intensity prior to the initial ^{13}C ϕ pulse, which can be set to the Ernst angle for optimum sensitivity/pulse repetition. Adiabatic 180° ^{13}C pulses produce better inversion profiles for resonances far from the offset frequency (such as quaternary carbonyl carbon resonances) compared with standard hard 180° inversion pulses. These ensure that maximum signal sensitivity is achieved both close to and far from the transmitter offset. Gradients can be chosen to select different categories of signals (see caption, **Figure 13**) and the ^{1}H θ pulse angle is set to define the editing profile within the data: $\theta = 45°$ yields all positive signals; $\theta =$

90° yields only resonances from CH centres and $\theta = 135°$ results in patterns typical of DEPT ^{13}C NMR data with the added bonus of signals from quaternary carbon centres being present.

3.4.2 ^{13}C-$\{^{1}H\}$-UDEFT

A modern take on the Driven Equilibrium Fourier Transform (DEFT)[28] is also helpful for enhancing 1D ^{13}C-$\{^1$H$\}$ NMR data. Originally designed to compensate for ^{13}C nuclei with particularly long T_1 relaxation times (*see* emrstm0054), DEFT allows significant shortening of the relaxation delay. It relies on a spin-echo, during the first half of which the ^{13}C FID is acquired. The second half of the echo is used to refocus still-evolving magnetization, which is then returned to the z-axis with a 90° pulse of opposite phase to that used in preparing the initial magnetization. In its original form DEFT was prone to all manner of imperfections arising from experimental set up including pulse mis-setting and field inhomogeneity effects causing the sequence to underperform and fall from favour. The modern version is UDEFT (Uniform Driven Equilibrium Fourier Transform, **Figure 14**)[29] in which the features responsible for previous under-performance are corrected. In particular, the method is tolerant to pulse mis-setting. The adiabatic 180° pulse inverts the sense of ^{13}C spin-vector rotation and after a period 2Δ, ^{13}C magnetization is precisely refocused. Application of the remaining $90°_x$-$180°_x$(adiabatic) sequence perfectly restores ^{13}C z-magnetization. The repetition time can be reduced to 3-5 s while generating quantitatively accurate data for nuclei with even the longest T_1 relaxation time constants. In the context of high-throughput laboratories, the technique is robust and can be used to replace the traditional power-gated ^{13}C-$\{^1$H$\}$ data acquisition scheme.

(Insert **Figure 14** here)

4   PULSE SEQUENCES FOR 2D NMR SPECTROSCOPY

Sophisticated and powerful as they can be, pulse sequences that generate one-dimensional NMR spectra are only a fraction of the solution-phase NMR methods as a whole. Multi-dimensional methods provide access to a richer wealth of data (*see* emrstm1181). Modern methods allow such data to be accumulated at accelerated rates with tremendous reliability and accuracy. These are considered under the separate headings of homo-nuclear and hetero-nuclear techniques.

4.1 2D homo-nuclear through-bond correlations

Classical two-dimensional homo-nuclear correlations are traditionally applied to non-dilute spins at natural abundance or to samples uniformly enriched in specific nuclei, a common feature of biomolecular NMR studies. They follow the general scheme *preparation-evolution-mixing-acquisition*. Preparation promotes spin relaxation, residual signal purging, restoration of z-magnetization and solvent signal handling. Evolution yields indirect chemical shift labelling of spins as a function of incremental delays. Mixing allows cross-talk between interacting spins and acquisition is the data collection period, which is increasingly taking on different forms in high-resolution liquids NMR[10] (also *see* emrstm1024).

4.1.1   COSY and TOCSY

Many variations of COSY (*see* emrstm0095 and emrstm0096) exist from the simplest two-pulse, non-phase sensitive experiment to sophisticated gradient selected, multiple quantum filtered, phase sensitive variants. Absolute value COSY data can be acquired with a single transient per t_1 increment (**Figure 15a**) making it ideal for quick acquisitions on abundant nuclei when there is sufficient signal.

(Insert **Figure 15** here)

The multiple quantum filtered analogue (**Figure 15b**) selects the coherence pathway on the basis of gradient ratios. Phase sensitive variants require the introduction of 180˚ pulses in association with gradient pulses to compensate for unwanted phase errors that arise through chemical shift evolution during the gradients. A zero quantum suppression scheme may also be incorporated using the approach described previously and is followed by a purging gradient (**Figure 15c**). For comparison, 2D-TOCSY yields strong responses with pure absorption lineshape, often revealing the identity of entire spin-system partners (*see* emrstm1165). Replacement of the selective r.f. pulse and related gradient pulse, g1, in **Figure 2b** with a t_1 incremental delay results in the generalized 2D-TOCSY with zero-quantum suppression. The results are analysed in partnership with COSY and edited-HSQC/HMQC data to reduce the information content when establishing neighbouring spin partner identities.

4.2 2D homo-nuclear through-space and chemical-exchange correlations

4.2.1   NOESY

Starting with the 1D-NOESY sequence (**Figure 4**), removing the selective pulse components along with their associated gradients and replacing these by a t_1 incremental delay similarly generates a pulse sequence suitable for 2D-NOESY data acquisition (also *see* emrstm0347 and emrstm0350). The addition of preceding pulse constructs during the preparation period or spin-echo components following the final read pulse allows ready adaptation of the sequence for solvent suppression. T_1 relaxation characteristics govern the choice of mixing time, τ_m, which, for small, non-aggregating molecules, typically lies in the range 0.5-1.0 s and for larger molecules ($M_r > 2$ kDa) in the range 0.05–0.20 s. 'Medium' sized molecules (1000<

M_r<2000), for which $\omega\tau_c \approx 1.12$ (where ω is the Larmor precession frequency and τ_c the molecular correlation time) require 2D-ROESY for NOE observation in the rotating frame of reference.

4.2.2 ROESY

In contrast to NOESY as a straightforward and reliable method, ROESY (*see* emrstm0473) has not been problem-free historically. The main issues have been data contamination caused by COSY and TOCSY cross-peaks (*see* emrstm0573) and cross-peak intensity distortions arising from resonance offset effects. Some pulse schemes were developed to circumvent these issues to increase the reliability of ROESY but no single method proved to be a cure-all for the issues encountered until a method dubbed EasyROESY was recently proposed and demonstrated[30].

(Insert **Figure 16** here).

EasyROESY uses adiabatic ramped pulses to transfer z-magnetization to and from the spin-lock axis at the beginning and end of each spin-lock period (**Figure 16**). The spin-lock offset frequency is shifted from a low value during the first half of the mixing period to a high value during the second half. Spin-lock frequency offsets are equally disposed about the transmitter offset and lie well outside the observation window, typical values being $\pm 5000 < \pm\nu_{\text{offset}} < \pm 6000$ Hz relative to a transmitter offset of 0 Hz. Purging gradients follow each spin-lock period. Using this approach, the offset dependency of the ROE signal intensity is eliminated and TOCSY artefacts are simultaneously reduced to a minimum. Resulting data are reliable for the purposes of integration and inter-nuclear distance measurement in molecules of medium size.

4.3 Relaxation Parameter and Diffusion Coefficient Measurement

Although not formally two-dimensional, T_1, T_2 and diffusion coefficient (D) parameter measurements follow some two-dimensional data acquisition principles. Time- or gradient-related parameters are systematically varied giving data attenuated as a function of the respective variable and stored as a two-dimensional array.

4.3.1 T_1 and T_2 measurement

T_1, the spin-lattice relaxation time constant, traditionally measured by means of an inversion recovery sequence $180°_x$–vd–$90°_x$–acq (vd is a variable delay) is determined by fitting relevant data to an expression of the form $I_t = I_0 + Pe^{-t/T_1}$ (where I_t is signal intensity at vd $= t$, I_0 is signal intensity at vd $= 0$ and T_1 is the longitudinal spin-lattice relaxation time constant). T_2 data emerge from the application of those sequences shown (**Figure 7**) and are fitted to expressions of the form $I_t = I_0(1- e^{-t/T_2})$, where T_2 is the transverse, spin-spin relaxation time constant. Although care needs to be taken in the choice of relaxation and inter-pulse delays, the methods are robust and easily implemented under automation.

4.3.2   DOSY (see emrstm0118 and emrstm0119)

By contrast, quantitative evaluation of diffusion coefficients, D, under automation can be fraught with difficulty, requiring careful choices and a conservative evaluation of results. The principal competing issue is convection, which owes its presence, in an NMR context, to the design of sample temperature regulation systems. Addition of a constant convection velocity to diffusive motion severely distorts the resulting NMR data giving unreliable diffusion parameters. Some physical adjustments can help to eliminate convection flow including reduced diameter NMR tubes, viscous solvents, lower temperatures and volume-restricted

samples. Convection compensation can also be incorporated within the relevant pulse program (**Figure 17**), which is consequently extended compared with related sequences.

(Insert **Figure 17** here)

This stimulated echo approach spatially encodes the magnetization and stores it along the z-axis. Spatial encoding with gradients uses the bipolar pulse pair (BPP) sequence, which minimizes deuterium lock signal disturbance and lineshape distortions in the final NMR data. For the convection compensated sequence shown, the self-diffusion period, Δ, is divided into two sections. Any phase error introduced by convection flow in the first half of the sequence is cancelled in the second. The delay, T_e, of typical duration 5 ms, promotes eddy current dissipation prior to data acquisition. Pulse sequences such as this require extensive phase cycling to eliminate unwanted signals, meaning considerable signal averaging, which is not always desirable especially for strong samples. The alternative Oneshot sequence only requires a single scan per spectrum[31](**Figure 18**).

(Insert **Figure 18** here)

Oneshot uses bipolar pulse pairs where the ramped gradients are unbalanced by a factor α such that $(|g1 - \alpha|) = (|g2 + \alpha|)$. The gradient imbalance is countered by ramped gradient $|g3| = 2\alpha$ applied during the diffusion period. The gradient imbalance dephases unwanted magnetization left over after application of the 180° pulses and also maintains lock stability. Purging gradients, g0, are applied as balanced pairs during the relaxation delay and within the diffusion period Δ, maintaining the exclusive presence of z-magnetization during the diffusion period. Using these techniques, data acquired in pseudo-2D format as a function

of gradient strength may be processed by regression fitting against the Stejskal-Tanner equation, modified where necessary depending on the pulse sequence used. 2D plots can be generated that carry chemical shift and diffusion coefficient information along orthogonal axes. Processing is technically non-trivial although this is mainly hidden behind user-friendly programs in most available software. The danger of this is that without care, false diffusion coefficient values can be interpreted as real. These can occur particularly for overlapped resonances or arise through the influence of chemical exchange. Methods such as PROJECTED (PROJECT Extended to DOSY)[32] can assist with the latter while the issue of resonance overlap may be addressed by combining DOSY and Pureshift methods to reduce the incidence of resonance overlap.[33]

4.4 2D hetero-nuclear correlations

Among the more powerful solution-phase NMR methods for small molecule structure elucidation, the data supply to automated structure verification (ASV) and the introduction of increased data resolution are those that yield information from correlations between different types of nuclei. This can be through either ${}^nJ_{HX}$-couplings or dipolar couplings in the form of the heteronuclear NOE. Modern techniques benefit from many historical refinements to give artefact-free, signal- and resolution-maximizing procedures. Virtually exclusive use is made of proton-detection, which amplifies signals by factors of up to several orders of magnitude compared with the results obtained through direct observation of the hetero-nuclear spin (*see* emrstm0209). Further incremental advances in sensitivity are incorporated by means of sensitivity improvement schemes and recently through the introduction of Pureshift methods designed to decouple homo-nuclear proton couplings in the directly detected dimension.[34] The greatest advance in the quality of data arising from all of these methods owes its success to pulsed field gradients (*see* emrstm0164). These are used to best effect when selecting only

the information required through gradient coherence selection. For organic molecules, this means the elimination of magnetization from protons attached either to spin-silent ^{12}C nuclei or quadrupolar spin-1 ^{14}N nuclei. This directly affects NMR spectrometer receiver gain: large responses that would otherwise be present from unwanted proton signals are eliminated prior to detection rather than being eliminated by phase-cycling following detection, thus allowing optimized digitization of signals. Pulsed field gradients also help to eliminate other artefacts including t_1 ridges and thus improve the overall quality of data.

4.4.1   One-bond heteronuclear correlations

HMQC and HSQC are most commonly used for detecting correlations between ^{1}H and other spin-½ nuclei, particularly ^{13}C and ^{15}N, *via* $^1J_{HX}$. An advantage of HMQC is its robustness towards mis-setting of pulse lengths as well as delivering a limited number of r.f. pulses, thus shortening the sequence overall relative to HSQC. ^{1}H homo-nuclear coupling evolves during the hetero-nuclear chemical shift evolution period, producing split cross-peaks in the indirectly detected dimension, a drawback if resolution is an issue. HSQC does not suffer from this effect but is a longer pulse sequence that is not insensitive to pulse mis-setting. One optimized HSQC sequence is the gradient selected version with sensitivity improvement and options for multiplicity-editing (**Figure 19**), throughout which ^{13}C adiabatic 180˚ pulses are used in place of 180˚ hard pulses.

(Insert **Figure 19** here)

The adiabatic CHIRP 180˚ pulses invert ^{13}C magnetization and exactly refocus $^1J_{HC}$ couplings of different sizes. Phase distortion artefacts that would arise from incomplete refocusing of $^1J_{HC}$ couplings are minimized and double reverse INEPT at the end of the

sequence generates sensitivity improvement.[35] The sequence can be tuned for the presence/absence and appearance of signals from CH, CH_2 and CH_3 groups by adjusting the delays Δ_x. For $\Delta_0 = 1/(2.^1J_{HC})$, CH and CH_3 signals appear inverted with respect to CH_2 signals. For $\Delta_2 = 1/(8.^1J_{HC})$, signals are present from all carbon types with the exception of quaternary carbons, whereas $\Delta_2 = 1/(4.^1J_{HC})$ gives only signals from CH groups. Gradient coherence selection is achieved by setting the gradient ratio $g1:g2 = \gamma_H:\gamma_X$, which for [^{1}H, ^{13}C] HSQC means a ratio of 4:1. Typically these gradients are at 80% and 20% of maximum strength and sufficient to suppress all unwanted magnetization arising from ^{12}C-attached ^{1}H nuclei. The conditions allow fast data acquisition with optimum digitization. Although complex in form, modern NMR systems are capable of handling the different elements of such a sequence with ease. Rapid calibration of pulse lengths under automation as described earlier make this method robust for operation without user intervention leading to excellent routine data generation. The classical elements of composite pulse decoupling (*see* emrstm0108) during the data acquisition period and ^{1}H decoupling *via* the 180° inversion pulse midway into the ^{13}C chemical shift evolution period ensure that data are presented as simply as possible. Pureshift approaches have recently yielded the Pureshift-HSQC[34] by which HSQC data are acquired with homo-nuclear broadband ^{1}H decoupling during the ^{1}H data acquisition period, along with ^{13}C broadband decoupling, in a segmented fashion that mirrors related methods. The data benefit by increased resolution in the ^{1}H dimension together with increased signal intensity. Where such techniques are implementable on modern NMR spectrometers, there is scope for simultaneous sensitivity and resolution improvement in routine data acquisition that should supersede many of the commonly adopted methods used for detecting hetero-nuclear $^1J_{HX}$ correlations.

4.4.2   Multiple-bond hetero-nuclear correlations

The partner to HMQC and HSQC is a method that correlates H and X through bonding networks according to $^{n}J_{HX}$ where n ≥ 2. This HMBC[36] (*see* emrstm1176) (**Figure 20**) achieves direct suppression of signals arising from $^{1}J_{HX}$ and operates similarly to HMQC by generating responses through hetero-nuclear double and zero-quantum coherence.

(Insert **Figure 20** here).

Correlation through multiple bonds relies on the evolution of long range $^{n}J_{HX}$ coupling during delay Δ_{LR}. Optional low-pass *J*-filters eliminate signals from $^{1}J_{HX}$ prior to the long range $^{n}J_{HX}$ coupling evolution period. The delays Δ_{1}-Δ_{3} are matched to the range of possible $^{1}J_{HX}$ coupling constants. Gradient ratios during the low-pass filter period sum to zero meaning that evolution of the long-range couplings remains unaffected. In the example, sensitivity is enhanced compared with related methods and pure absorption lineshapes are generated in the indirectly detected dimension along with gradient coherence selection. Mixed lineshape is maintained in the directly detected dimension meaning that HMBC data must be presented in magnitude mode. In general for HMBC, no advantage is gained by decoupling the hetero-nucleus during signal detection. Long-range $^{n}J_{HX}$-couplings revealed through HMBC are small (in the range 2-7 Hz) compared with the equivalent one-bond coupling constants. As Δ_{LR} corresponds to $1/(2.^{n}J_{HX})$ for n ≥ 2, this creates delays of typically 70-250 ms during the pulse sequence, which can be problematic if transverse relaxation plays a significant part. Widely differing values of Δ_{LR} are required to capture correlations associated with the possible range of small sized $^{n}J_{HX}$ values meaning more than one data set with different values of Δ_{LR} must be acquired. An alternative approach in the form of ACCORDIAN spectroscopy enables long range couplings of different sizes to be revealed in a single data set.[37] HMBC and related methods do not immediately distinguish between $^{2}J_{HX}$, $^{3}J_{HX}$ or $^{4}J_{HX}$,

these often being of similar size to one another. Care as well as judgement is therefore required for correct data interpretation. As a compromise, H2BC was devised to exclusively select correlations from $^2J_{HX}$ couplings.[38] This works by first exploiting $^1J_{HC}$ followed by $^3J_{HH}$ and is equivalent to running the concatenated sequence HMQC-COSY. The method is only suitable for revealing correlations where proton-attached hetero-nuclei are involved.

4.4.3   HSQC-TOCSY

2D HSQC-TOCSY extends this idea (*see* emrstm0467). Here the acquisition stage of the HSQC is replaced by a spin-lock construct. ^1H magnetization previously labelled with hetero-nuclear chemical shift information during the HSQC segment is spin-locked during the TOCSY mixing period. The effect is to propagate X-filtered ^1H magnetization to the associated spin-system partners under the condition of strong coupling brought about by the spin-lock. The resulting data show spin-system-related proton resonance networks at each hetero-nuclear chemical shift associated with each related proton. The technique disperses overlapped ^1H spin-systems along the orthogonal hetero-nuclear chemical shift dimension in a manner that cannot be matched using 2D [^1H, ^1H] TOCSY alone. When combined with data from 2D [^1H, ^1H] TOCSY and COSY, multiplicity-edited 2D [^1H, X] HSQC and 2D [^1H, X] HMBC, the 2D [^1H, X] HSQC-TOCSY can provide key confirmatory signal assignment evidence and is an invaluable tool in the NMR specialist's armoury.

4.4.4   HOESY

HOESY is the final pulse sequence to be considered here. Like the homo-nuclear NOE, the hetero-nuclear Overhauser effect (hetero-nuclear NOE) occurs through a dipolar coupling mechanism between different types of nuclei, one of which is usually proton. The experiment (**Figure 21**) may be carried out in either hetero-nuclear-or proton-detected modes.

(Insert **Figure 21** here)

Choice in this is governed by sensitivity, resolution, T_1 relaxation times and solvent considerations. ^{1}H-detection is preferable in the case of lower γ nuclei including ^{13}C and ^{15}N whereas some merit exists in X-nucleus detection, particularly if measuring hetero-nuclear NOEs between ^{1}H and ^{19}F nuclei.[39] The added advantage of this for aqueous samples is that solvent suppression can be avoided. Particular care must be taken over the choice of mixing time in this context. ^{19}F T_1 relaxation times can be similar in size to ^{1}H T_1s but may be considerably shorter or considerably longer. The pulse sequence can be adapted in a number of ways including the incorporation of a spoiling gradient within the mixing period and adaptation as a gradient-selected procedure. The latter is particularly useful since the hetero-nuclear NOE response is small and non-gradient-selected data can result in large artefacts arising from t_1 ridges.

5   CONCLUSIONS

In this article I have highlighted pulse sequences that are current and routinely used within the setting of pharmaceutical or chemical NMR laboratories but I have also provided a nod towards those developing techniques that show significant promise for the future. While solution-phase sequences have formed the focus here, the importance of solid-state methods is not diminished given the consideration required of the solid state form in many of the materials that are studied in a pharmaceutical development context. The methods noted are meant to provide a toolkit of sequences that might be suitable for robust, routine, unsupervised, automated use but which are capable of providing top quality, reproducible results. The development of new pulse sequences, incremental improvements in tried and

tested methods and the revival of old procedures given a new twist due to modern hardware developments is a constant theme in the evolving field of NMR spectroscopy. My hope is that this article provides sufficient information for the reader to gain some knowledge of how the described techniques can benefit their work as well as providing some impetus to go further in exploring the much wider landscape of NMR methods.

References

1. M. Weiger, T. Speck and M. Fey, *J. Magn. Reson.*, 2006, **182**, 38.

2. P. A. Keifer, *Concepts Magn. Reson.,*1999, **11**, 165.

3. P. S. C. Wu and G. Otting, *J. Magn. Reson.*, 2005, **176**, 115.

4. O.W. Sørensen, M. Rance and R. R. Ernst, *J. Magn. Reson.*, 1984, **56**, 527.

5. J. Keeler, *Understanding NMR Spectroscopy*, John Wiley and Sons, Chichester, 2005, p. 415

6. D. Uhrín, in *Methods for Structure Elucidation by High-Resolution NMR: Applications to Organic Molecules of Moderate Molecular Weight*, eds. G. Batta, K. Kover and C Szantay Jr., Elsevier Science, Amsterdam, 1997, pp. 51-89.

7. A. J. Pell, R. A. Edden and J. Keeler, *Magn. Reson.Chem.*, 2007, **45**, 296.

8. L. Castañar, P. Nolis, A. Virgili and T. Parella, *Chem. Eur. J.*, 2013, **19**, 17283.

9. J. A. Aguilar, S. Faulkner, M. Nilsson and G. A. Morris, *Angew. Chem. Int. Ed.*, 2010, **49**, 3901.

10. N. H. Meyer and K. Zangger, *Angew. Chem. Int. Ed.,* 2013, **52**, 7143.

11. M. Foroozandeh, R. W. Adams, N. J. Meharry, D. Jeanerat, M. Nilsson and G. A. Morris, *Angew. Chem. Int. Ed.*, 2014, **53**, 6990.

12. J. A. Aguilar, A. A. Colbourne, J. Cassani, M. Nilsson and G. A. Morris, *Angew. Chem. Int. Ed.*, 2012, **51**, 6460.

13. V. M. R. Kakita and J. Bharatam, *Magn. Reson. Chem.*, 2014, **52**, 389.

14. J. Ying, J. Roche and A. Bax, *J. Magn. Reson.*, 2014, **241**, 97.

15. J. A. Aguilar, M. Nilsson, G. Bodenhausen and G. A. Morris, *Chem. Comm.*, 2012, **48**, 811.

16. M. Piotto, V. Saudek and V. Sklenár, *J. Biomol. NMR*, 1992, **2**, 661.

17. T.-L. Hwang and A. J. Shaka, *J. Magn. Reson. Ser. A*, 1995, **112**, 275.

18. M. Liu, X. Mao, C. Ye, H. Huang, J. K. Nicholson and J. C. Lindon, *J. Magn. Reson.*, 1998, **132**, 125.

19. S. H. Smallcombe, S. L. Patt and P. A. Keifer, *J. Magn. Reson. Ser. A*, 1995, **117**, 295.

20. S. B. Shuker, P. J. Hajduk, R. P. Meadows and S. W. Fesik, *Science*, 1996, **274**, 1531.

21. B. Meyer and T. Peters, *Angew. Chem. Int. Ed.*, 2003, **42**, 864.

22. D. W. Begley, S. O. Moen, P. G. Pierce and E. R. Zartler, *Curr. Protocols in Chem. Biol.*, 2013, **5**, 251.

23. C. Dalvit, P. Pevarello, M. Tato, M. Veronesi, A. Vulpetti and M. Sundström, *J. Biomol NMR*, 2000, **18**, 65.

24. C. Dalvit, G. Fogliatto, A. Stewart, M. Veronesi and B. Stockman, *J. Biomol NMR*, 2001, **21**, 349.

25. R. Burger and P. Bigler, *J. Magn. Reson.*, 1998, **135**, 529.

26. S. L. Patt and J. N. Shoolery, *J. Magn. Reson.*, 1982, **46**, 535.

27. P. Bigler, R. Kümmerle and W. Bermel, *Magn. Reson. Chem.*, 2007, **45**, 469.

28. E. D. Becker and T. C. Farrar, *J. Am. Chem. Soc.*, 1969, **91**, 7784.

29. M. Piotto, M. Bourdonneau, K. Elbayed, J.-M. Wieruszeski and G. Lippens, *Magn. Reson. Chem.*, 2006, **44**, 943.

30. C. M. Thiele, K. Petzold and J. Schleucher, *Chem. Eur. J.*, 2009, **15**, 585.

31. M. D. Pelta, G. A. Morris, M. J. Stchedroff and S. J. Hammond, *Magn. Reson. Chem.*, 2002, **40**, S147.

32. J. A. Aguilar, R. W. Adams, M. Nilsson and G. A. Morris, *J. Magn. Reson.*, 2014, **238**, 16.

33. M. Nilsson and G. A. Morris, *Chem. Comm.* 2007, 933.

34. L. Paudel, R. W. Adams, P. Király, J. A. Aguilar, M. Foroozandeh, M. J. Cliff, M. Nilsson, P. Sándor, J. P. Waltho and G. A. Morris, *Angew. Chem. Int. Ed.*, 2013, **52**, 11616.

35. P. K. Mandal and A. Majumdar, *Concepts Magn. Reson.*, 2004, **20A**, 1.

36. D. O. Cicero, G. Barbato and R. Bazzo, *J. Magn. Reson.*, 2001, **148**, 209

37. G. E. Martin and C. E. Hadden, *Magn. Reson.Chem.*, 2000, **38**, 251.

38. N. T. Nyberg, J. Ø. Duus and O. W. Sørensen, *J. Am. Chem. Soc.*, 2005, **127**, 6154.

39. J. Battiste and R. A. Newmark, *Prog. Nucl. Magn. Reson. Spectrosc.*, 2006, **48**, 1.

Further Reading

High-resolution NMR techniques in Organic Chemistry, ed. T. D. W. Claridge, Elsevier

Science Ltd., Oxford, 1999.

Biographical Sketch

John A. Parkinson. b. 1964. BSc. 1985, PhD., 1989, Leeds: Applications in NMR

spectroscopy; Postdoc., University of Manchester, 1989; Edinburgh-based National

Ultra-high field NMR facility 1990, later associating with the Metals-in-Medicine

Group at the same institute. Appointed NMR Spectroscopist, University of

Strathclyde, 2001, promoted to Senior Research Fellow, 2013. Approx. 160

collaborative research articles on applications of solution phase NMR spectroscopy.

Research interests: (bio)molecular structure elucidation, recognition and assembly;

enzyme reaction profiling; mixture analysis; nucleic acids.

Tables and Captions

Figures Captions

Figure 1 Gradient echo imaging sequence where the total gradient strengths for g1 and g2 are

equal and TE_1 and TE_2 are gradient echo periods used to acquire different data sets. ^1H

represents the r.f. channel where narrow black rectangles relate to 90° hard pulses. G_z relates

to pulsed field gradients.

Figure 2 1D-TOCSY pulse sequences. **a)** Classical 1D-TOCSY using a DIPSI-2 spin-lock

and z-filters. **b)** 1D-TOCSY sequence adapted to eliminate contributions from zero-quantum

coherence pathways. The trapezoidal pulses with diagonal arrows represent frequency swept smoothed CHIRP adiabatic 180˚ pulses applied over spatially encoding gradients, g0, with values 1-3% of maximum z-gradient strength.

Figure 3 Example data for 1D-TOCSY. **a)** Region of data as reference acquired using a single pulse-acquire scheme. **b)** Equivalent region to **a)** but acquired with selective inversion of signal at δ^1H = 5.8 ppm using pulse sequence shown in **Figure 2a**. **c)** Equivalent region to **a)** but acquired by selective inversion of the same resonance at δ^1H = 5.8 ppm using pulse sequence shown in **Figure 2b**.

Figure 4 Typical scheme for 1D-NOESY where τ_m is the mixing time.

Figure 5 Pulse sequence for band-selective ^{1}H-$\{^1$H$\}_{REG}$ NMR spectra (REG = region-selection). The boxed element consists of an interrupted acquisition stage by which data are acquired between r.f./gradient pulse elements. Complete data acquisition with homo-nuclear decoupling is achieved over n-cycles of the acquisition stage.

Figure 6 H1′/H5 resonance region of the ^{1}H NMR spectrum of a nucleic acid sample. **a)** Standard 1D ^{1}H NMR spectrum; **b)**^{1}H NMR spectrum acquired using HOBS sequence shown in **Figure 5**. **c)** ^{1}H NMR spectrum acquired using instantaneous Pureshift. **a)** and **b)** were acquired with 16 transients whereas **c)** was acquired with 8192 transients.

Figure 7 Spin echo. **a)** Classical CPMG pulse sequence - the bracketed sequence is repeated n times to promote loss of signal through T_2 relaxation. **b)** PROJECT pulse sequence where n > 1. Wide vertical bars represent 180° refocusing pulses.

Figure 8 T_2-editing. **a)** ^{1}H NMR spectrum of human blood serum edited using the pulse sequence shown in **Figure 7b**. **b)** Reference 1D ^{1}H NMR spectrum.

Figure 9 Presaturation pulse sequence variants. The standard procedure is shown as the main figure. Content in the bracketed region may be replaced by **a)** 1D NOESYPRESAT; **b)** composite 90˚ degree read pulse; **c)** saturation period followed by spoiling gradient and 90˚ read pulse; **d)** spoiling gradient followed by composite 90˚ read pulse.

Figure 10 WET. Gradient ratio g1:g2:g3:g4 = 80:40:20:10. ^{13}C decoupling takes place during each pulse and the acquisition period if organic solvents are used. The read pulse is presented as a composite 90˚ pulse.

Figure 11 WET applied to a mixture of solutes dissolved in 60% H_2O, 40% CH_3CH_2OH **a)** in the absence and **b)** presence of ^{13}C-decoupling according to the scheme of **Figure 10**. Note the ^{13}C doublet of quartet satellites * for the methylene proton signal of the ethanol solvent in **a)**. ^{13}C satellites of the CH_2 signal mask resonances from solute molecules, which are only revealed when WET is applied with ^{13}C decoupling during application of the selective pulse elements.

Figure 12 Water-LOGSY

Figure 13 DEPTQ. ϕ and θ indicate pulses of variable length, $\Delta = 1/(2J_{XH})$ and the trapezoids show adiabatic 180° refocusing pulses. g1 = g2 = g3 yields all carbon signals, g1 = 0, g2 = g3 yields only CH_n (no quaternary) and g1 = g2 ≠ g3 yields only quaternary carbon signals.

Figure 14 UDEFT. Data acquisition occurs following the first 90° pulse. Adiabatic pulses are used to precisely refocus and invert ^{13}C spin-magnetization allowing short recycle times. ^{1}H decoupling may be applied throughout as shown in this example.

Figure 15 COSY. **a)** Gradient-accelerated absolute value COSY. **b)** Multiple quantum filtered absolute value COSY: g1 is set for either 16% (double quantum filter) or 4% (triple quantum filter) when g2 and g3 are set to 12% and 40% respectively. **c)** z-COSY with zero-quantum suppression. The small flip angle pulses (θ_1 and θ_2) give rise to z-COSY cross-peak and diagonal structures.

Figure 16 EasyROESY. Adiabatic ramped pulses are represented by the curves at either end of the spin-lock periods identified as SL low and SL high.

Figure 17 Convection compensated stimulated echo diffusion pulse sequence. Ramped gradients are shown with diagonal arrows. Δ is the diffusion period and T_e a delay to allow for eddy current dissipation.

Figure 18 Oneshot DOSY

Figure 19 Fully optimized gradient selected, multiplicity-edited, phase sensitive 2D [^{1}H, ^{13}C] HSQC.

Figure 20 Gradient-selected HMBC with optional 3-fold low-pass $^1J_{HX}$ filter (bracketed region)

Figure 21 Basic HOESY configured for direct detection of the hetero-nuclear response.

Figures
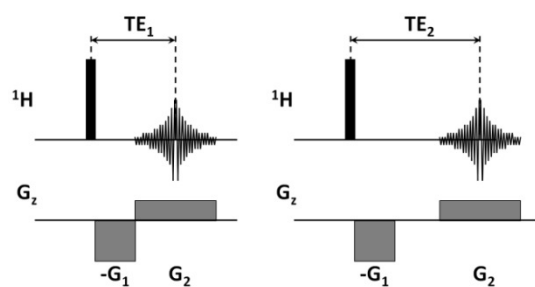
Figure 1
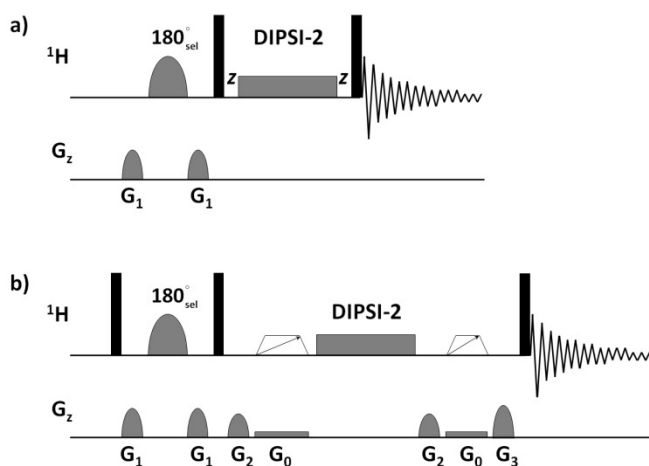
Figure 2
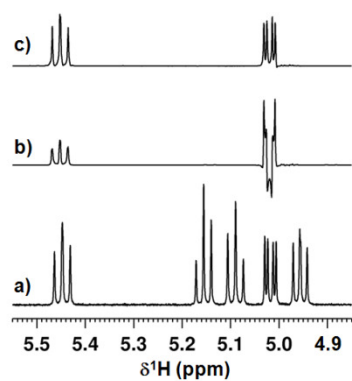
Figure 3
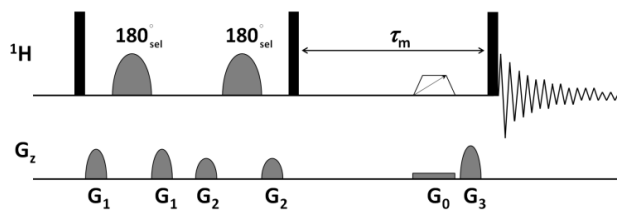
Figure 4
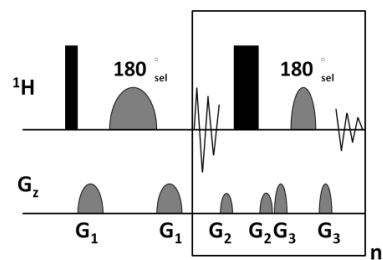
Figure 5
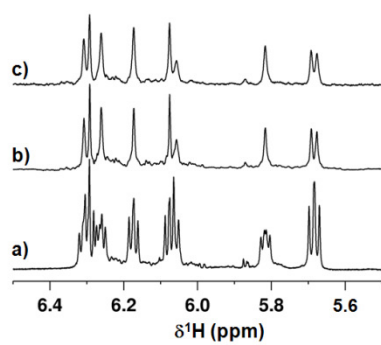
Figure 6
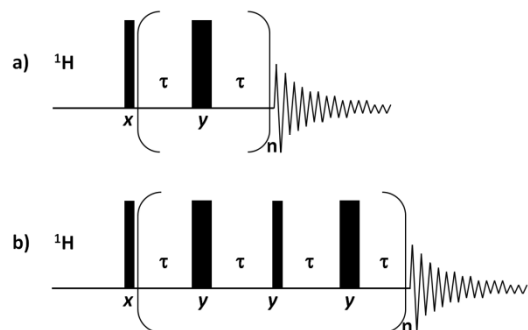
Figure 7
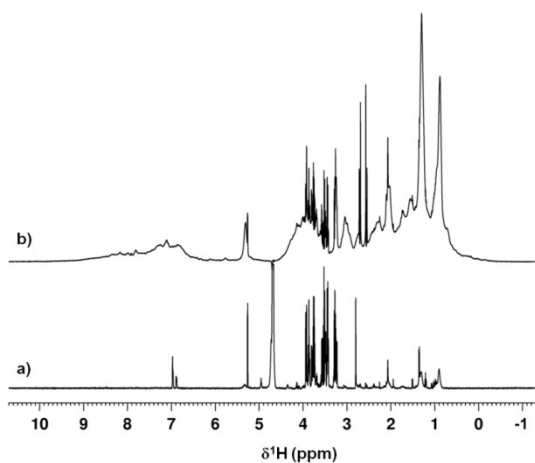
Figure 8
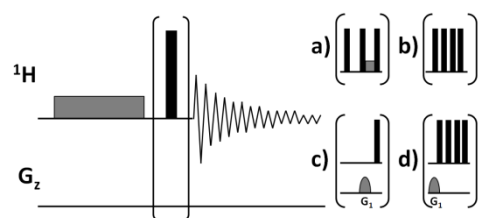
Figure 9
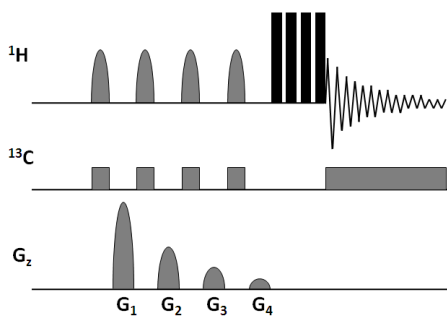
Figure 10
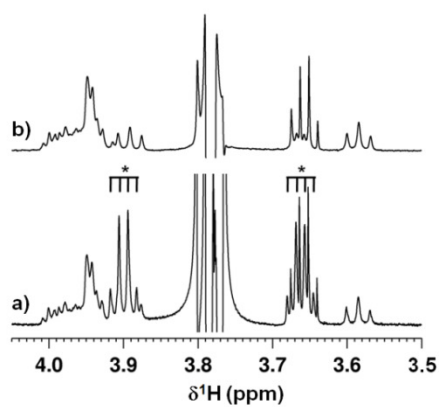
Figure 11
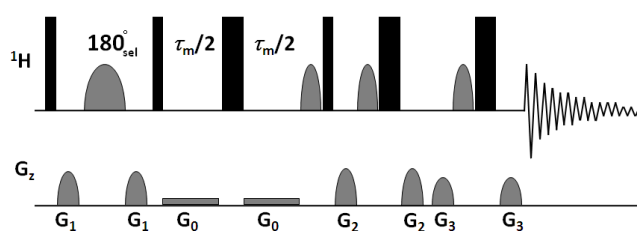
Figure 12
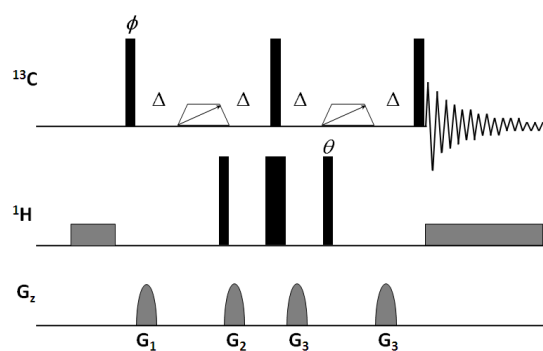
Figure 13
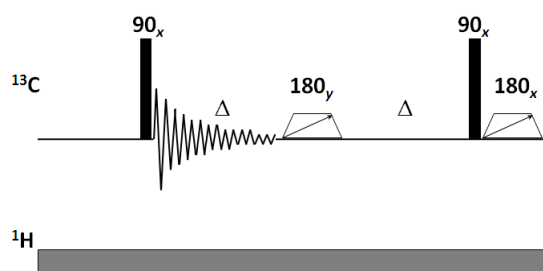
Figure 14
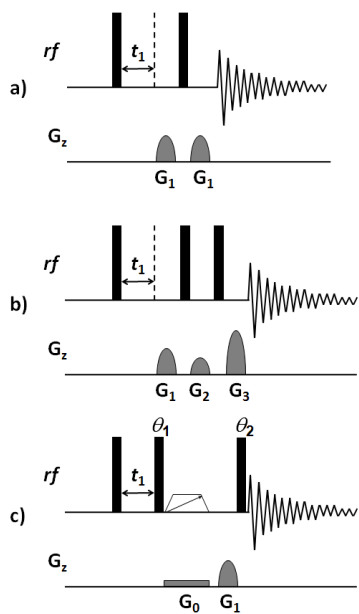
Figure 15
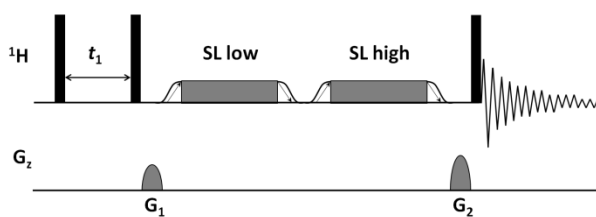
Figure 16
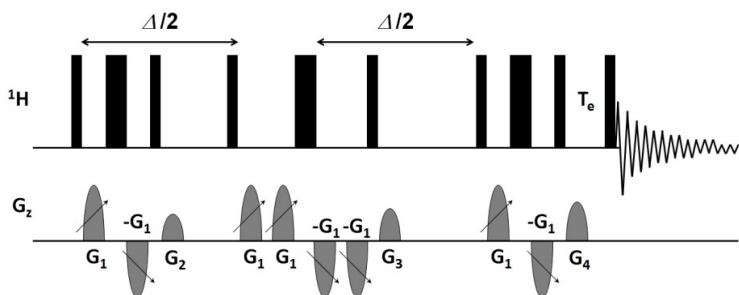
Figure 17
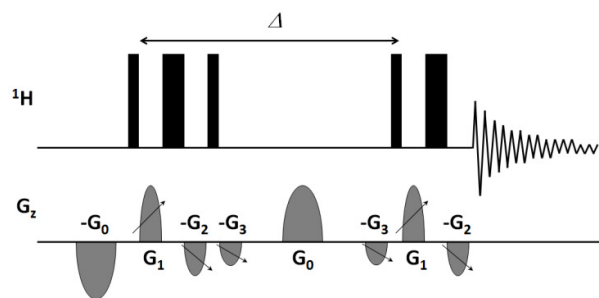
Figure 18
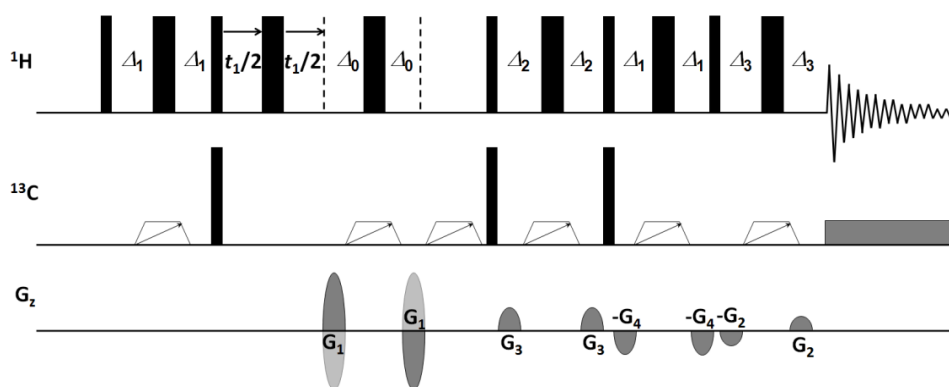
Figure 19

Figure 20

Figure 21